Available online at www.sciencedirect.com
ScienceDirect
Nuclear Instruments and Methods in Physics Research B 258 (2007) 388–394
NIM B
Beam Interactions with Materials & Atoms
www.elsevier.com/locate/nimb

Radiostability of butylated hydroxytoluene (BHT): An ESR study

H. Tuner *, M. Korkmaz

Department of Physics Engineering, Faculty of Engineering, Hacettepe University, Beytepe, Ankara 06800, Turkey

Received 15 November 2006; received in revised form 23 February 2007
Available online 2 March 2007

Abstract

In the present work, the effects of gamma radiation on solid butylated hydroxytoluene (BHT), which is used as an antioxidant, were investigated by ESR spectroscopy. While unirradiated BHT presented no ESR signal, irradiated BHT exhibited an ESR spectrum with many resonance maxima and minima spread over a magnetic field range of 12 mT and centered at about $g = 2.0026$. Weak satellite and central intense resonance lines, likely, originated from radical species of different stabilities and ratios were observed to be responsible from experimental ESR spectrum of gamma irradiated BHT. Studies based on the variations of the observed line intensities and spectrum area under different experimental conditions were carried out and characteristic features of the radical species responsible from experimental ESR spectrum were determined. Mesomeric radical species of different stabilities providing to BHT a G value of 0.25 were believed to be induced in gamma irradiated BHT. While species responsible from weak satellite lines were unstable, the species causing central intense lines were found to be relatively stable. BHT belongs to a class of compounds with low radiosensitivity ($G = 0.25$). This feature of BHT enables the feasibility of radiosterilizations of the products containing BHT as antioxidant without very much loss from its antioxidant benefit. BHT has been shown to provide an opportunity in the estimation of applied radiation dose with a reasonable accuracy if an appropriate mathematical function is used to describe experimental dose-response data.

PACS: 61.72.Cc; 87.50.Gi; 87.64.Hd

Keywords: Butylated hydroxytoluene (BHT); Electron spin resonance; Antioxidant; Irradiation

1. Introduction

Butylated hydroxytoluene (BHT), or chemically 2,6-di-*tert*-butyl-*p*-cresol, is a fat soluble organic compound primarily used as an antioxidant food additive (E321) [1–3]. It is also used as an antioxidant in cosmetics, pharmaceutical drugs, jet fuels, rubber and petroleum products. BHT slows down the rate of autoxidation in foods and prevents changes in the foods colour, odour and taste by reacting with free radicals. It can be added to the food itself or to the packing materials. BHT prevents oxidative rancidity of fats. It is also added directly to shortening, cereals and other foods containing fats and oils. However, the same chemical properties making BHT excellent preservatives may also implicate in health effects [4–9]. The oxidative characteristics and/or metabolites of BHT may contribute to carcinogenicity or tumorigenecity [10–12]. Certain persons may have difficulty in metabolizing BHT resulting in health and behaviour changes. BHT may also have antiviral and antimicrobial activities. Oxygen reacts preferentially with BHT rather than oxidizing fats and oils, thereby protecting them from spoilage.

Radiostability of BHT is important from its effectiveness point of view in the case of sterilization by radiation of materials such as foods, pharmaceutical drugs, cosmetics etc. containing it as preservative. Thus, the aim of the present work is to study the radiation stability of solid BHT through a detailed ESR study carried out on the kinetic, spectroscopic and dosimetric features of the radiolytic intermediates produced in it after gamma irradiation.

* Corresponding author. Tel.: +90 312 297 72 13; fax: +90 312 299 20 37.
E-mail address: htuner@hacettepe.edu.tr (H. Tuner).

0168-583X/$ - see front matter © 2007 Elsevier B.V. All rights reserved.
doi:10.1016/j.nimb.2007.02.098

2. Materials and methods

BHT samples were provided from GMT Food Ingredients (Istanbul) and HUNCA Cosmetics (Istanbul) companies and were stored at room temperature in a well-closed container protected from light and humidity. No further purification was performed, that is, it was used as it was received. BHT is a white crystalline or flaked solid, odourless or having a characteristic faint aromatic odour. It is insoluble in water, but is freely soluble in alcohol. Its melting point is about 342–345 K and it has a molecular structure as given in Fig. 1. It is made of low atomic number element as in the case of soft tissue. Samples with particle sizes smaller than 1 μm were used throughout the experiment to avoid orientation dependent effects on recorded spectra. All irradiation were performed at room temperature using a ^{60}Co gamma cell supplying a dose rate of 1.41 kGy/h as an ionising radiation source at the Sarayköy Establishment of Turkish Atomic Energy Agency in Ankara. The dose rate at the sample sites was measured by a Fricke dosimeter. Investigations were performed on sample irradiated at nine different doses (1, 2, 3, 5, 7, 10, 15, 25 and 34 kGy).

ESR measurements were carried out on samples in standard quartz ESR tubes using BRUKER EMX 131 X-band spectrometer operating at 9.8 GHz and equipped with a high sensitive cylindrical microwave cavity. Signal intensity were calculated, both, from first derivative spectra and compared with that obtained for a standard sample (DPPH) under the same spectrometer operating conditions and from double integration of the recorded first derivative spectra. Sample temperature inside the microwave cavity was monitored with a digital temperature control system (BRUKER ER4131-VT). This unit provided the opportunity of measuring the temperature with an accuracy of ±0.5 K at the site of sample inside the microwave cavity. A cooling, heating and subsequent cooling cycle was adopted to monitor the evolutions of the ESR line shape with temperature using samples irradiated at room temperature at a dose of 10 kGy. Variations in the spectrum pattern and in the resonance line intensities with microwave power at room (290 K) and at 130 K were also studied in the range of 0.005–2.5 mW and 0.001–1.0 mW, respectively.

Kinetic behaviours at 330 K, 335 K, 337.5 K and 340 K of the contributing radical species were determined through annealing studies. To achieve this goal, the samples irradiated at room temperature were heated inside the microwave cavity to predetermined temperatures and kept at these temperatures for predetermined time, than, their ESR spectra were recorded. The results were presented as the average of five replicates for each radiation dose.

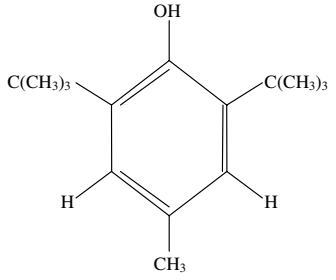

Fig. 1. Molecular structure of BHT.

3. Experimental results and discussion

3.1. General features of the ESR spectra, variation with applied dose and microwave power

No ESR signal was observed for unirradiated BHT. However, BHT irradiated at room temperature exhibited an ESR spectrum spread over a magnetic field range 12 mT and centred at about $g = 2.0026$. It consisted of many resonance lines (Fig. 2(a) and (b)) obviously divided into intense central lines and weak satellite lines which are symmetrical positioned at low and high field sides of four intense central lines. Numbers were assigned to maxima and minima of experimental spectrum (Fig. 2(a) and (b)) and all evaluations were made in accordance with this assignment. From their intensity difference it was concluded that intense and weak lines originate from the presence of at least two different radical species of different structure and concentration in gamma irradiated BHT. The pattern difference between spectra recorded just after (Fig. 2(a)) and 160 days after (Fig. 2(b)) irradiation were considered as a clear indication of the presence of more than one radical species exhibiting different room temperature stability characteristics. Separations of the resonance lines among intense and weak groups were calculated to be different and to vary in the magnetic field ranges of 1.07–1.20 mT and 0.75–0.90 mT, respectively. Increase in the absorbed dose caused increases in the intensities of central and satellite lines without creating pattern changes in the studied dose range (1–34 kGy). However, as it will be emphasized in the next sections, drastic pattern changes occurred in the experimental spectra of sample at about melting point of BHT.

Variation of the signal intensities associated with spectrum maxima and minima, which were measured with respect to spectrum base line and normalized to the receiver gain, the mass of the sample and the intensity of the standard, with applied microwave power were studied both at room temperature (290 K) and at 130 K. The results relevant to intense resonance lines are presented in Fig. 3(a) and (b). The rates of saturation are different. This indicates that even in the formation of intense resonance lines, more than one radical species are responsible just after the radiation.

3.2. Variable temperature results

Temperature is an important parameter in the determination of kinetic and spectroscopic features of radical species. Thus, possible variations in the ESR spectrum pattern

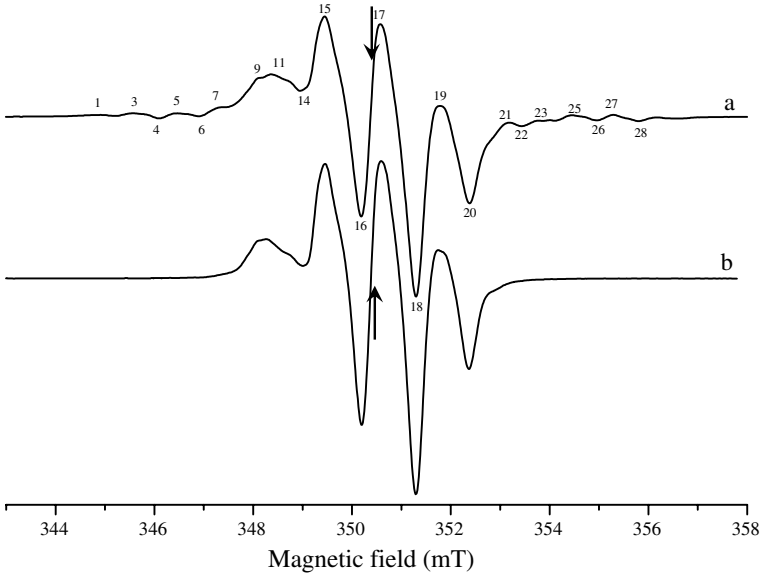

Fig. 2. Experimental spectra recorded (a) just after irradiation and (b) 160 days after irradiation. Arrows indicate the position of DPPH resonance line ($g = 2.0036$).

and signal intensities of gamma irradiated BHT were studied over a large temperature range. Cooling samples down to 130 K produced no change in the spectrum pattern except reversible Curie changes in the peak to peak intensities of the studied central resonance lines (Fig. 4). However, increase in the temperature above room temperature produced irreversible decrease in these intensities (Fig. 4) up to melting point of BHT (342–345 K) where a drastic pattern change, possibly associated with the change in the delocalization of unpaired electron on the benzene ring, was observed to occur (Fig. 5). As is seen from the last figure, this new spectrum obviously originates from the interaction of unpaired electron with two sets of equivalent protons. First, three equivalent protons split resonance line into four lines of the rotation 1:3:3:1, than, two other equivalent protons split, in their turn, these lines into three lines of the ratio 1:2:1. An ESR spectrum of this intensity is expected to originate from radical species of high concentration, likely, produced upon the transformation of the species induced in BHT after gamma irradiation rather than species created thermally. In a separate experiment, an ESR spectrum of the same pattern and same hyperfine splitting but barely detectable with the used ESR spectrometer (EMX 131) was observed to be induced in BHT heated up to its melting point and kept at this temperature for ten minutes.

3.3. Stabilities of the radical species at room temperature

Room temperature stabilities of the radical species are important for irradiation dose measurement by ESR spectroscopy. Thus, long term room temperature stabilities of the species responsible from experimental spectrum of gamma irradiated BHT were investigated by recording spectrum in regular time interval over a storage period of more then five months (160 days). The results relevant to the evolutions of the 27–28 and 17–18 peak to peak signal intensities and spectrum area over this storage period are given in Fig. 6 as an example for these evolutions. It is seen that, while weak lines tend to decrease continuously over the storage period of about two months, intense lines experience continuous increases over a storage period of about forty days, likely, due to the transformation of a part of the radical species responsible from weak lines to species giving rise to intense lines while the rest decaying in the same period. Although, weak lines disappeared almost completely at the end of the first two months of the storage, intense lines experienced a very slight decrease beyond this period. Fast decay of the species associated with weak resonance lines at the beginning of storage period (Fig. 6), that is, during nearly the first six days of storage was observed to cause a relatively fast decrease in the spectrum area. At the end of this period, spectrum area still continued to decrease but with another decay rate, that is, nearly with the decay rate of the species responsible from central intense lines. This was considered implying the existence of two different process taking place after the first six days of storage: transformation of the species associated with weak lines to those associated with central intense lines and the decays of the latter species.

3.4. Radical kinetics at high temperature

Radical species are expected to decay faster at high temperatures due to increase in the molecular motions. To test this idea and to determine kinetic features and diffusional activation energies of the contributing radical species at high temperatures, annealing studies were performed at four different temperatures (330 K, 335 K, 337.5 K and 340 K) below melting point of BHT. It was not possible

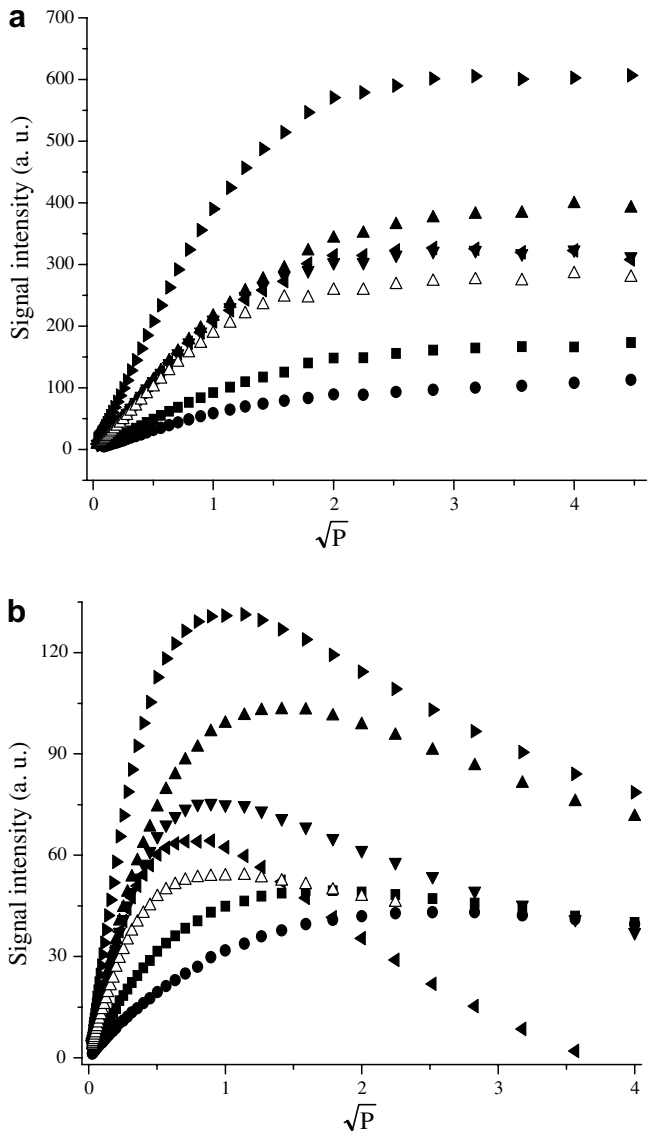

Fig. 3. Variations of the assigned intensities, measured with respect to spectrum base line, with applied microwave power at two different temperatures. (a) Room (290 K); (b) 130 K. 11 (■); 14 (●); 15 (▲); 16 (▼); 17 (◀); 18 (▶); 20 (Δ).

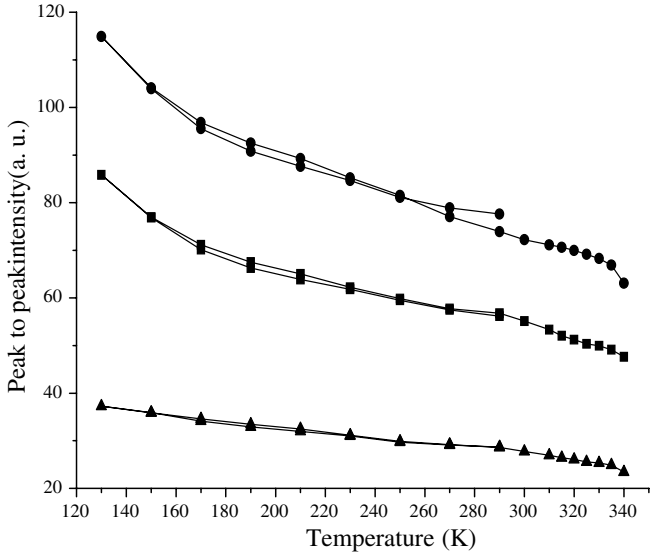

Fig. 4. Variations of the peak to peak intensities with temperature in the range of 130–340 K. 15–16 (■); 17–18 (●); 19–20 (▲).

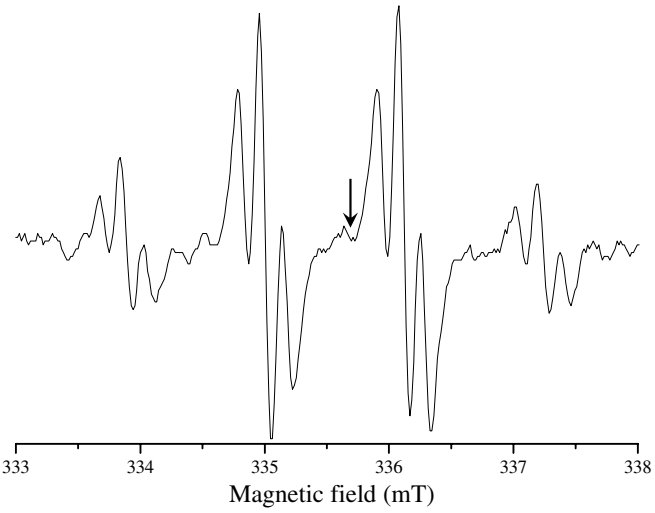

Fig. 5. Spectrum obtained when irradiated sample was heated up to 345 K. Arrow indicates the position of DPPH resonance line ($g = 2.0036$).

to carry out reliable annealing studies related with low and high field weak lines due to high uncertainty in their intensity determination and unstability of the radical species responsible from them. Instead, annealing studies were performed using central intense lines freed from contribution of unstable species. That is, the intensities obtained for central intense lines for samples stored at room temperature for a long time (160 days) (Fig. 2(b)) were used for this purpose. The results associated with the peak to peak intensity for 17–18 resonance line (Fig. 2(a)) are given in Fig. 7 as an example for performed annealing studies. Similar evaluations were done for 11–14; 15–16; 19–20 central resonance lines, but they are not given here to save space. A mathematical function of the form $I = a + b \cdot \exp(-(kt)$ was found to describe best experiment signal intensity decay data derived for 11–14; 15–16; 17–18; 19–20 resonance lines at all annealing temperatures. Decay constants calculated by this technique are given in Table 1. Calculated decay constants were used to get diffusional activation energy of the involved radical species and a value of $E = 71.8 \pm 2.2$ kJ/mol was found from $\ln(k) - \frac{1}{T}$ plot.

3.5. Dosimetric features of BHT

Sensitive and accurate dose measurement can be achieved by ESR technique if radiosensitivity of irradiated substance is high. A higher concentration of radical species generated at the same absorbed dose of radiation, indicates a higher sensitivity of the substance toward the type of radiation used. Therefore, dosimetric features of

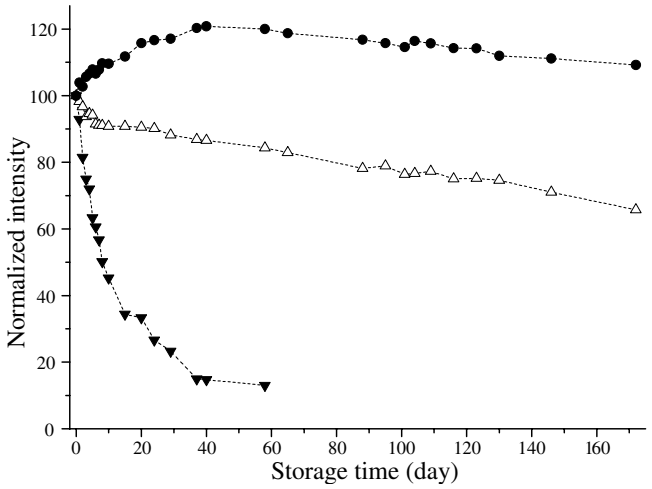

Fig. 6. Variations of the peak to peak intensities and spectrum area with storage time at room temperature. Weak line 27–28 (▼); intense line: 17–18 (●); spectrum area (Δ).

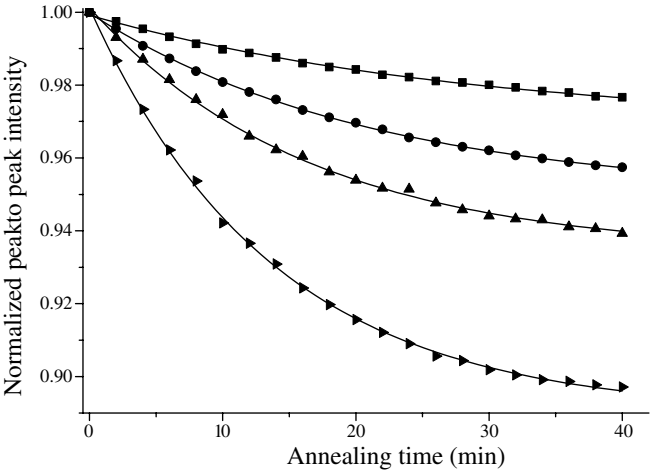

Fig. 7. Variations of the peak to peak intensities corresponding to the assigned line 17–18 with annealing time and annealing temperature. 330 K (■); 335 K (●); 337.5 K (▲); 340 K (▶).

Table 1
Decay constants calculated from annealing studies of central intense lines

Temperature (K)	Decay constant $k \times 10^5$ (min^{-1})	Correlation coefficient (r^2)
330	3405	0.99748
335	4731	0.99968
337.5	6059	0.99841
340	7301	0.99941

BHT were also studied through the variations of the central line intensities and spectrum area with absorbed gamma radiation dose in a wide range (1–34 kGy). Uncertainties in the determination of the intensities of weak resonance lines and relatively fast decay of the species responsible from these lines discouraged us performing dosimetric studies based on these species. Samples of ground BHT irradiated to doses of 1, 2, 3, 5, 7, 10, 15, 25 and 34 were used to construct the experimental dose-response curves relevant to central resonance lines. It is important to emphasize once more that in the studied dose range (1–34 kGy) the positions and the relative distances between studied resonance lines did not change nor did other lines appear. A G value of 0.25 compatible with those obtained for aromatic molecules, was calculated for gamma irradiated BHT by comparing the spectrum area of a sample irradiated at a dose of 5 kGy with the area derived for a standard sample of known spin number ($n = 5.2 \times 10^{16}$ spin/kg).

Critical to an accurate and reliable estimate of the dose is the choice of mathematical expression used to describe the dose-ESR response curve. The mathematical functions given in Table 2 were tried to describe the variations of the intensities of resonance lines 15–16; 17–18 and 19–20 derived from spectra recorded just after irradiation with absorbed radiation dose without forcing the functions to pass through origin. In these functions, I and D stand for the ESR line intensity and absorbed dose in kGy, respectively, and a, b, c, etc. are the constants to determine. These functions have been mentioned previously [13–20] for the estimation of the absorbed dose in radiation processed foods and pharmaceutical drugs. As can be seen from Table 2 power and linear function including a quadratic term describe best experimental intensity data obtained for interested resonance lines. However, the intercept, which reflect the intensity at zero applied dose, is relatively high for linear function including a quadratic term although its correlation coefficients are all higher for evaluated three resonance lines. Theoretical dose-response curves calculated using parameter values given in Table 2

Table 2
Mathematical functions used to describe experimental dose-response data in the range of 1–34 kGy and calculated parameters

Function		Resonance line		
		15–16	17–18	19–20
Linear $I = a + bD$	a	−0.05124	−0.37451	0.45151
	b	2.12048	2.86894	1.03029
		(0.99393)	**(0.99548)**	**(0.99230)**
Linear + quadratic	c	2.14955	2.14655	0.92551
$I = c + dD + qD^2$	d	1.58261	2.25280	0.69375
	q	0.01598	0.01830	0.01000
		(0.99826)	**(0.99858)**	**(0.99950)**
Power $I = f\,D^{g}$	f	1.77533	2.37241	0.69905
	g	1.05463	1.05692	1.11344
		(0.99511)	**(0.99670)**	**(0.99618)**
Exponential	h	4282.52254	9528.07193	8526.93827
$I = h(1\text{-}e^{-jD})$	j	0.00050	0.00030	0.00012
		(0.99363)	**(0.99524)**	**(0.99145)**
Sum of two	k	1043.97763	41560.24428	2855.22884
exponentials	m	0.00082	0.00003	0.00018
$I = k(1 - e^{-mD})$	n	1479.68997	40985.74630	2795.93214
$+ n(1 - e^{-pD})$	p	0.00087	0.00003	0.00018
		(0.99340)	**(0.99539)**	**(0.99138)**

Figures in the brackets are the related correlation coefficients.

for linear function including a quadratic term are also represented as solid lines, with their experimental counterparts in Fig. 8. As is seen from this figure, 15–16; 17–18 and 19–20 resonance lines increase up to about 15 kGy linearly, but above this dose, they experience a slight deviation from linearity. 17–18 line is the most sensitive among others to the gamma radiation.

To be used as a dosimetric material, one must be able to predict the irradiation dose from mathematical function(s) used to describe its dose response data. The utility of proposed mathematical function best describing experimental dose-response data, that is $I = a + bD + cD^2$ function, was tested by calculation of interpolated doses. Briefly, back-calculated or interpolated doses were obtained by entering the measured signal intensities in the mathematical function comprising a linear and a quadratic dose terms. The results are presented in Table 3 for 15–16; 17–18; and 19–20 resonance lines. Differences between applied (D_a) and calculated (D_c) doses were presented as percent ratios

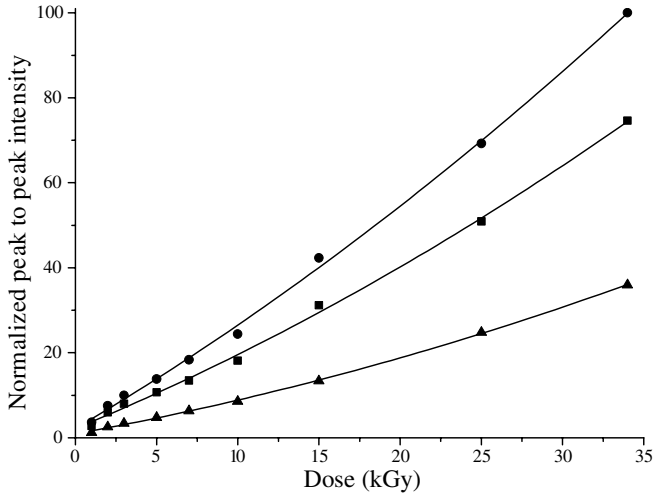

Fig. 8. Dose response curves. Symbol: experimental, 15–16 (■); 17–18 (●); 19–20 (▲), solid line: theoretical; calculated from $I = a + bD + cD^2$ function.

Table 3
Applied doses calculated by entering the measured signal intensities of three intense central lines in the $I = a + bD + cD^2$ function

Applied doses (kGy)	Calculated doses (kGy)		
	Resonance lines		
	15–16	17–18	19–20
1.0	0.382 −[0.62]	0.664 −[0.34]	0.404 −[0.60]
2.0	2.342 [0.17]	2.339 [0.17]	2.254 [0.13]
3.0	3.592 [0.20]	3.385 [0.13]	3.419 [0.14]
5.0	5.131 [0.03]	4.985 [0.00]	5.171 [0.03]
7.0	6.698 −[0.04]	6.807 −[0.03]	7.116 [0.02]
10.0	9.259 −[0.07]	9.186 −[0.08]	9.652 −[0.03]
15.0	15.821 [0.05]	15.793 [0.05]	14.818 −[0.01]
25.0	24.669 −[0.01]	24.802 −[0.01]	25.222 [0.01]
34.0	34.082 [0.00]	34.030 [0.00]	33.930 [0.00]

Figures in the brackets are the percent differences between applied (D_a) and calculated (D_c) doses defined as $\eta = \frac{D_a - D_c}{D_a}$.

($\eta = \frac{D_a - D_c}{D_a}$) to give an idea about the deviations. It is seen that applied radiation doses can be estimated with an accuracy of better than eight percent in the dose range of 5–34 kGy by using a linear function of the applied dose containing a quadratic dose term.

4. Conclusion

Gamma irradiated BHT exhibits an ESR spectrum with many resonance lines which can be divided into two subgroups: intense central and weak satellite lines. The latters are symmetrically positioned at both sides of formers. While species responsible from weak satellite lines decays relatively fast at room temperature (290 K), species given rise to intense central lines is quite stable at 290 K. Spectrum pattern is independent from applied dose and sample temperature in the range of 1–34 kGy and 130–340 K, respectively, but above 342 K a drastic change in the pattern implying the ESR spectrum of a radical species in solutions occurs. Intense central lines display different microwave saturation characteristics at room temperature and at 130 K (Fig. 3(a) and (b)).

The decreases and increases in the intensities of the weak satellite and central lines (Fig. 6), respectively, over the first 40 days of storage at room temperature was considered as an indication of the decay and, in large extent, the transformation of isomeric radical species responsible from weak satellite lines into species causing central intense lines beside a slight decay of the latter species. The results of the annealing studies performed at high temperatures (330 K, 335 K, 337.5 K and 340 K) reveal that a single radical species having a diffusional activation energy of 71.8 ± 2.2 kJ/mol is responsible from central intense lines. Unpaired electron of the long life species was believed to interact with two sets of unequivalent protons, that is, three methyl and two ring protons. Fast motion of the methyl group about C–C bond [21] likely makes the protons of this group equivalent. In melted samples, localization of the unpaired electron is changed and the latter is supposed to spend most of its time on the benzene ring. Gamma irradiated BHT is calculated to have a G value (0.25) similar to those obtained for aromatic molecules such as benzene and naphthalene. This means that radiosensitivity of BHT toward gamma radiation is low and that it can be used as an antioxidant in radiosterilized cosmetics, pharmaceutical drugs etc. without very much loss from its antioxidant efficiency. Although, it is a compound with poor radiosensitivity, BHT has been shown to provide the opportunity of estimation of applied radiation dose with a reasonable accuracy in the dose range of 5–34 kGy (Table 3).

References

[1] D.V. Parke, D.F. Lewis, Safety aspects of food preservatives, Food Addit. Contam. 9 (5) (1992) 561.
[2] K.B. Schwarz, Oxidative stress during viral infection: a review, Free Radical Bio. Med. 21 (5) (1996) 641.

[3] C. Lerlercq, D. Arcella, A. Turrini, Estimates of the theoretical maximum daily intake of erythorbic acid, gallates, buthylated hydroxyanisole (BHA) and buthylated hydroxytoluene (BHT) in Italy: a stepwise approach, Food Chem. Toxicol. 38 (12) (2000) 1075.
[4] J.P. Klein, T.R. Van Vleet, J.O. Hall, R.A. Coulombe Jr., Effects of dietary buthylated hydroxytoluene on aflatoxin B(1)-relevant metabolic enzymes in turkeys, Food Chem. Toxicol. 41 (5) (2003) 671.
[5] O. Meyer, E. Hansen, Behavioural and developmental effects of buthylated hydroxytoluene dosed to rats in utero and in the lactation period, Toxicology 16 (3) (1980) 247.
[6] A.M. Safer, A.J. al-Nughamish, Hepatotoxicity induced by the antioxidant food additive, buthylated hydroxytoluene (BHT), in rats: an electron microscopical study, Histol. Histopathol. 14 (2) (1999) 391.
[7] C.M. Siman, U.J. Eriksson, Effect of butylated hydroxytoluene on alpha-tocopherol content in liver and adipose tissue of rates, Toxicol. Lett. 87 (2–3) (1996) 103.
[8] M. Takami, S.L. Preston, V.A. Toyloy, H.R. Behrman, Antioxidants reversibly inhibit the spontaneous resumption of meiosis, The Am. J. Physiol. 276 (4) (1999) E684.
[9] R.J. Xiu, A. Freyschuss, X. Ying, L. Berglund, P. Henriksson, I. Björkhem, The antioxidant butylated hydroxytoluene prevents early cholesterol-induced microcirculatory changes in rabbits, J. Clin. Invest. 93 (6) (1994) 2732.
[10] T. Umemura, Y. Kodama, K. Hioki, T. Nomura, A. Nishikawa, M. Hirose, Y. Kurokawa, The mause rasH2/BHT model as an in vivo rapid assay for lung carcinogens, Jpn. J. Cancer Res. 93 (8) (2002) 861.
[11] A.M. Malkinson, Lung Tumor Promation by BHT, Crisp Data Base National Institutes of Health, 1999.
[12] G.M. Williams, M.J. Iatropoulos, Inhibition of the hepatocarcinogenicity of aflatoxin B1 in rats by low levels of the phenolic antioxidants buthylated hydroxyanisole and buthylated hydroxytoluene, Cancer Lett. 104 (1) (1996) 49.
[13] N.J.F. Dodd, J.S. Lea, A.J. Swallow, ESR detection of irradiated food, Nature 334 (1988) 387.
[14] M.F. Desrosiers, G.L. Wilson, C.R. Hunter, D.R. Hutton, Estimation of the absorbed dose in radiation-processed food-1. Test of the EPR response function by a linear regression analysis, Appl. Radiat. Isot. 42 (1991) 613.
[15] M.F. Desrosiers, Estimation of the absorbed dose in radiation-processed food-1. Test of the EPR response function by an exponential fitting analysis, Appl. Radiat. Isot. 42 (1991) 617.
[16] M.A. Ghelawi, J.S. Moore, R.H. Bisby, N.J.F. Dodd, Estimation of absorbed dose in irradiated dates (*Phoenix dactylifera* L.). Test of ESR response function by a weighted linear least-squares regression analysis, Radiat. Phys. Chem. 60 (2001) 143.
[17] S. Tepe, M. Polat, M. Korkmaz, Effects of radiation on carbapenems: ESR identification and dosimetric features of gamma irradiated solid meropenem trihydrate, Radiat. Eff. Defect S. 161 (11) (2006) 653.
[18] J.P. Basly, I. Basly, M. Bernard, Electron spin resonance identification of irradiated ascorbic acid: dosimetry and influence of powder fineness, Anal. Chim. Acta 372 (1998) 373.
[19] M. Polat, M. Korkmaz, Effect of gamma radiation on amlodis and its potential for radiosterilization, J. Pharmaceut. Biomed. 40 (4) (2006) 882.
[20] E.M. Stewart, Detection methods for irradiated foods, in: R.A. Molins (Ed.), Food Irradiation: Principles and Applications, John Wiley & Sons, New York, 2001.
[21] J.M. Polson, J.D. Dean Fyfe, K.R. Jeffrey, The reorientation of *t*-buthyl groups in buthylated hydroxytoluene: a deuterium nuclear magnetic resonance spectral and relaxation time study, J. Chem. Phys. 94 (5) (1991) 3381.